HHS Public Access

Author manuscript

Neurobiol Aging. Author manuscript; available in PMC 2017 May 01.

Published in final edited form as:

Neurobiol Aging. 2016 May ; 41: 25–38. doi:10.1016/j.neurobiolaging.2016.02.004.

Aging is associated with dimerization and inactivation of the brain-enriched tyrosine phosphatase STEP

Sathyanarayanan Rajagopal[*], **Ishani Deb**[*], **Ranjana Poddar**, and **Surojit Paul**[#,¶]

University of New Mexico Health Sciences Center, Department of Neurology, 1 University of New Mexico, Albuquerque, NM – 87131

[#]Department of Neurosciences, 1 University of New Mexico, Albuquerque, NM – 87131

Abstract

The striatal-enriched tyrosine phosphatase (STEP) is involved in the etiology of several age-associated neurological disorders linked to oxidative stress and is also known to play a role in neuroprotection by modulating glutamatergic transmission. However, the possible effect of aging on STEP level and activity in the brain is still unclear. In this study, using young (1 month), adult (4 month) and aged (18 month) rats we show that aging is associated with increase in dimerization and loss of activity of STEP. Increased dimerization of STEP is primarily observed in the cortex and hippocampus and is associated with depletion of both reduced and total glutathione levels, suggesting an increase in oxidative stress. Consistent with this interpretation studies in cell culture models of glutathione depletion and oxidative stress also demonstrates formation of dimers and higher order oligomers of STEP that involves intermolecular disulfide bond formation between multiple cysteine residues. Conversely, administration of N-acetyl cysteine, a major antioxidant that enhances glutathione biosynthesis, attenuates STEP dimerization both in the cortex and hippocampus. The findings indicate that loss of this intrinsic protective response pathway with age-dependent increase in oxidative stress may be a contributing factor for the susceptibility of the brain to age-associated neurological disorders.

Keywords

Tyrosine phosphatase; STEP; dimerization; aging; glutathione; N-acetyl cysteine

[¶]Corresponding Author: Surojit Paul, PhD, University of New Mexico Health Sciences Center, Department of Neurology, 1, University of New Mexico, Albuquerque, NM – 87131, Tel: (505) 272-0610, Fax: (505) 272-8306, spaul@salud.unm.edu.
[*]These two authors have contributed equally to this work.

Disclosure statement for authors

The authors declare that they have no conflicts of interest.

1. INTRODUCTION

Aging is characterized by a progressive decline in the efficiency of physiological function and by the increased susceptibility to disease and death. Although the fundamental mechanisms are still poorly understood, a growing body of evidence points towards oxidative stress as one of the primary determinants of aging (Hagen, 2003; Kregel and Zhang, 2007). Oxidative stress induced redox imbalance has been associated with aberrant alteration in the tyrosine phosphorylation of key signaling proteins implicated in the pathogenesis of aging and many age-related neurodegenerative disorders (Schmitt et al., 2005; Droge and Schipper, 2007; Jung et al., 2009). The regulation of tyrosine phosphorylation involves agonistic and antagonistic activity of protein tyrosine kinases (PTKs) and protein tyrosine phosphatases (PTPs). Although a considerable amount of research has investigated the regulation of PTKs with oxidative stress and aging, our knowledge about the regulation of PTPs with aging is limited (Jin and Saitoh, 1995; Minetti et al., 2002; Schmitt et al., 2005; Wegiel et al., 2011).

The tyrosine phosphatase STEP (STriatal-Enriched Phosphatase) that is expressed exclusively in the central nervous system is emerging as an important regulator of neuronal function (Lombroso et al., 1993; Boulanger et al., 1995). The STEP-family of PTPs includes both membrane associated ($STEP_{61}$) and cytosolic ($STEP_{46}$) variants (Bult et al., 1997). Biochemical and electron microscopic studies have localized $STEP_{61}$ to endoplasmic reticulum, mitochondria, synaptic vesicles and post-synaptic densities (Bult et al., 1996). An emerging body of evidence indicates that the alteration in STEP function is associated with the progression of several age-associated acute and chronic neurological disorders including Alzheimer’s disease, Parkinson’s disorder and cerebral ischemia (Kurup et al., 2010; Deb et al., 2013; Xu et al., 2014; Kurup et al., 2015). An increase in STEP level and activity resulting from a disruption of the proteasomal degradation machinery is thought to interfere with synaptic strengthening resulting in cognitive and behavioral deficits observed in Alzheimer’s disease (Kurup et al., 2010). In contrast, lower STEP level and activity due to rapid degradation of the protein has been implicated in ischemia-induced brain damage (Deb et al., 2013). Thus it appears that both high and low level of STEP could disrupt cellular function resulting in neurodegeneration. Despite this evidence for a role of STEP in age-associated neurological disorders, a causal link between STEP and aging has still not been established.

A series of molecular and biochemical studies have found that the activity and stability of STEP is regulated by several post-translational modifications (Paul et al., 2000; Paul et al., 2003; Deb et al., 2011; Mukherjee et al., 2011). Reversible phosphorylation of a regulatory serine residue (Ser 221 in $STEP_{61}$/Ser 49 in $STEP_{46}$) in a conserved domain termed kinase interacting motif (KIM) has been shown to modulate STEP activity in terms of its ability to bind to its substrates (Paul et al., 2000; Paul et al., 2003). Additional studies investigating the regulation of ubiquitin-mediated proteasomal degradation of STEP found that phosphorylation of two SP/TP sites in a second conserved domain termed as kinase specificity sequence are important in maintaining the stability of STEP (Mukherjee et al., 2011). Another potentially important finding is that H_2O_2 induced oxidative stress leads to significant increase in the oligomerization of STEP in neurons resulting in substantial loss of

its enzymatic activity (Deb et al., 2011). Since aging is associated with an increase in oxidative stress, the present study sought to investigate the effect of aging on STEP dimerization in the brain and its association with the glutathione (GSH) levels, a major antioxidant that functions to maintain intracellular redox equilibrium.

2. METHODS

2.1. Materials and reagents

Male Sprague-Dawley rats (1, 4 and 18–20 month) were obtained from Harlan Laboratories (Livermore, CA, USA). Antibodies used were as follows: monoclonal anti-STEP from Novus Biologicals (Littleton, CO, USA), monoclonal anti-V5 from Invitrogen (Carlsbad, CA, USA), polyclonal PSD-95 from Cell Signaling, monoclonal anti-cMyc and polyclonal Calnexin from Santa Cruz (Santa Cruz, CA, USA), monoclonal anti-β-tubulin and polyclonal synaptophysin from Sigma (St. Louis, MO, USA). All secondary antibodies were from Cell Signaling. Protein G Sepharose was from GE Healthcare. N-acetyl cysteine (NAC), Diethylmaleate (DEM) and *para*-nitrophenylphosphate (pNPP) were from Sigma-Aldrich (St. Louis, MO, USA). GSH assay kit was from Arbor assays (Ann Arbor, MI, USA). All tissue culture reagents were obtained from Invitrogen. Approval for animal experiments was given by the University of New Mexico, Health Sciences Center, Institutional Animal Care and Use Committee.

2.2. Detection of dimers and oligomers using non-reducing SDS-PAGE

To detect the dimers and higher order oligomers of STEP both brain tissue and transfected cells were processed as reported previously (Deb et al., 2011). Briefly, cortical, hippocampal and striatal tissues were homogenized in a lysis buffer containing 50 mM Tris-HCl, pH 7.5, 100 mM NaCl, 1% Nonidet P-40 and cocktail of protease inhibitors, incubated on ice for 45 min and then centrifuged at 13,000 rpm for 10 min. For cell line experiments, cells were washed with PBS and then scraped in the lysis buffer, incubated on ice for 45 min and then centrifuged at 13,000 rpm for 10 min. Equal protein from each sample were diluted 1:1 with 2x Laemmli sample buffer, with β-mercaptoethanol (reducing conditions) or without β-mercaptoethanol (non-reducing conditions). The samples processed under reducing conditions were boiled for 10 min. The reducing and non-reducing samples were separated onto 7.5% or 6% SDS-polyacrylamide gels respectively. The proteins in the gel were transferred to polyvinylidene difluoride membrane and processed for immunoblot analysis.

2.3. Immunoblotting

Protein concentration in lysates was estimated using a bicinchoninic acid (BCA) protein assay kit (Thermo Scientific, Rockford, IL, USA). Equal amounts of protein from each sample was resolved by SDS-PAGE and transferred to polyvinylidene difluoride membrane. After blocking with 5% non-fat dry milk or BSA, membranes were incubated for 1 hr at room temperature or overnight at 4°C with the appropriate primary antibody. Horseradish peroxidase (HRP) coupled to anti-rabbit or anti-mouse IgG raised in goat were used as secondary antibodies. Immune complexes were detected on X-ray films after treatment with West Pico supersignal chemiluminescence reagents (Thermo Scientific). Densitometric analysis of immunoblots was performed using Image J software (http://rsbweb.nih.gov/ij/)

2.4. Glutathione assay

Glutathione (GSH) levels in brain homogenates were measured as described previously (Candelario-Jalil et al., 2007) with some modifications. Briefly, cortical, striatal or hippocampal slices were sonicated in PBS (pH 7.0) and then centrifuged at 13,000 rpm for 10 min at 4°C. The supernatant was processed for protein estimation using BCA kit. Equal amount of protein from each sample (30 μg) was incubated with equal volume of 5% sulfosalicylic acid (SSA) for 10 min in ice, followed by centrifugation at 13,000 rpm for 10 min. The supernatant was then diluted with the supplied assay buffer to bring the concentration of SSA to 1% and then incubated with ThioStar reagent in a black 96-well plate (total volume 50 μl) for 15 min at room temperature to determine the reduced GSH level. Fluorescent signal from each well was quantified spectrofluorometrically (Leica, Buffalo Grove, IL) using excitation and emission wavelengths of 390 and 510 nm, respectively. For quantitation of total GSH level, GSH reductase and NADPH reaction mixture were added to the wells followed by another 15 min incubation at room temperature and spectrofluorometric reading of the signal. Tissue GSH concentration was determined using a GSH standard curve.

To determine GSH levels following DEM or H_2O_2 treatment, HEK293 cells were washed twice with PBS, scraped with 0.1ml 2.5% SSA, incubated for 10 min on ice and then centrifuged at 13,000 rpm for 10 min (Dasgupta et al., 2005). The supernatant was used for GSH assay as described above. The resulting pellet was dissolved in 1x sample buffer (without β-mercaptoethanol), boiled for 10 min, centrifuged for 10 min at 13000 rpm. The supernatant was processed for protein assay to normalize GSH values against total protein.

2.5. Tyrosine phosphatase assay

Cortical tissue was homogenized in a buffer containing 50 mM Tris-HCl, pH 7.4, 150 mM NaCl and 1% NP-40 followed by centrifugation at 13,000 rpm for 10 min to collect supernatant for immunoprecipitation with anti-STEP antibody. Equal amount of protein from each sample (1.5 – 2 mg) was processed for immunoprecipitation with anti-STEP antibody (Deb et al., 2011). The immune complexes bound to protein G beads were then washed three times in a buffer containing 50 mM Tris-HCl, pH 7.4, 150 mM NaCl and 0.1% NP-40 and then once in a buffer containing 30 mM HEPES (pH 7.4) and 120 mM NaCl. For phosphatase assay the beads were incubated for 30 min at 30°C in 100 μl of reaction buffer (30 mM HEPES, pH 6.0, 150 mM NaCl, 10 mM pNPP) and reaction was stopped by addition of 0.9 ml of 0.2 N NaOH. Phosphatase activity of $STEP_{61}$ was measured by colorimetric quantitation of the formation p-nitrophenolate at 410 nm using a spectrophotometer (Deb et al., 2011). To assess the amount STEP immunoprecipitated the immune complexes bound to the beads were eluted with SD sample buffer and processed for immunoblot analysis with anti-STEP antibody. For cell line experiments, cells were lysed in a buffer containing 50 mM Tris-HCl, 150 mM NaCl and 0.1% NP-40, centrifuged at 13,000 rpm for 10 min, collect supernatant for immunoprecipitation with anti-V5 antibody. The samples were then processed for pNPP assay as mentioned above. The values obtained were normalized for the amount of STEP immunoprecipitated (Toledano-Katchalski et al., 2003; Deb et al., 2011).

2.6. Immunoprecipitation

Cells were lysed in a buffer containing 50 mM Tris-HCl, pH 7.4, 150 mM NaCl, 50 mM NaF, 10 mM $Na_4P_2O_7$, 1 mM Na_3VO_4, 0.1% NP-40 and protease inhibitor cocktail (Boehringer). Lysates were centrifuged for 10 min at 13,000 rpm to remove insoluble material, and then pre-cleared with protein G sepharose for 1 hr. For immunoprecipitation of STEP, samples were incubated overnight with anti-V5 antibody at 4°C. The immune complexes were incubated with protein G sepharose for 2 hr at 4°C. Beads were collected by centrifugation at 1000 rpm for 2 min and washed three times with lysis buffer. Proteins were eluted using SDS-sample buffer (Laemmli sample buffer with β-mercaptoethanol) and processed for SDS-PAGE and immunoblot analysis with antibodies as described in the individual experiments.

2.7. Cell culture and stimulation

Full-length $STEP_{61}$-cDNA was cloned into the pcDNA3.1/Myc-His and pcDNA 3.1/V5-His mammalian expression vectors (Invitrogen). Point mutants of $STEP_{61}$ were obtained by polymerase chain reaction (PCR) based site-directed mutagenesis (Stratagene, La Jolla, CA, USA). All mutations were verified by nucleotide sequencing. HEK293 cells obtained from A.T.C.C. were routinely grown in DMEM/F12, supplemented with 10% fetal bovine serum, at 37°C in a humidified atmosphere consisting of 5% CO_2 and 95% air. Cells were transiently transfected with 1 μg DNA using Lipofectamine™ 2000 (Invitrogen). After 24 hr cells were treated with 0 – 50μM of DEM for 6 hr or 10mM of H_2O_2 for 5 min in serum free minimal essential medium at 37°C. Cells were then processed for GSH assay, co-immunoprecipitation experiments or total SDS-polyacrylamide gel electrophoresis (SDS-PAGE) and immunoblot analysis under reducing or non-reducing conditions.

2.8. Subcellular fractionation of rat brain tissues

Biochemical fractionation was performed as described previously (Dunah and Standaert, 2001) with minor modifications. Briefly, cortical tissue from 1 old SD rats were homogenized in TEVP buffer (10 mM Tris-HCl, pH 7.4, 5 mM NaF, 1 mM Na_3VO_4, 1 mM EDTA, and 1 mM EGTA) containing 320 mM sucrose and was centrifuged for 10 min at 800g to remove nuclei and large debris (P1). The supernatant (S1) was centrifuged for 15 min at 9,200g to obtain the crude synaptosomal fraction (P2). The P2 fraction was re-suspended and incubated in a hypo-osmotic buffer (10 mM Tris-HCl, pH 7.4, 5 mM NaF, 1 mM Na_3VO_4, 1 mM EDTA, and 1 mM EGTA) containing 35.6 mM sucrose for 30 min and then centrifuged at 25,000g for 20 min to pellet the synaptosomal membrane fraction (LP1). The resulting supernatant (LS1) was centrifuged for 2 hr at 165,000g to obtain the synaptic vesicle-enriched fraction (LP2). The supernatant S2 was centrifuged at 165,000g for 2 hr to obtain the cytosolic fraction (S3) and a light membrane/microsome-enriched fraction (P3). After each centrifugation the resulting pellet was rinsed briefly with ice-cold TEVP buffer before subsequent fractionations to avoid possible crossover contamination. All centrifugations were performed at 4°C.

2.9. Drug treatment

Aged (18–20 month) SD rats were injected intraperitoneally with N-acetyl cysteine (50 mg/kg, dissolved in PBS) daily for two weeks. N-acetyl cysteine (NAC) was dissolved in PBS and made fresh at the beginning of each experiment. Control animals were injected with PBS daily for 2 weeks. 24 hr after the last injection one group of drug treated and control rats were processed for enzymatic evaluation of glutathione (GSH) level in the cortex and hippocampus. Another set of drug treated and control rats were processed for immunoblot analysis under both reducing and non-reducing conditions.

3.0. Data Analysis

Data in the text and figures are expressed as mean ± SEM. Statistical differences between multiple groups were assessed using one-way ANOVA followed by Bonferroni's *post hoc* comparison test. For statistical differences between two groups analysis was done using Student's *t* test. Differences were considered statistically significant when $p < 0.05$.

3. RESULTS

3.1. Aging is associated with increased dimerization of $STEP_{61}$

To examine the effect of age on dimerization of STEP, cortical, hippocampal and striatal tissues from young (1 month), adult (4 month) and aged (18 month) male SD rats were processed for immunoblot analysis with anti-STEP antibody under non-reducing condition. The results showed an age-dependent migration (upward shift in electrophoretic mobility) of $STEP_{61}$ to a position that corresponds to double the molecular weight (100–150 kDa) compared with $STEP_{61}$ monomer (61 kDa; Fig. 1, upper panel), suggesting the formation of dimers of $STEP_{61}$. A significant increase in dimerization of $STEP_{61}$ was observed only in the cortical (6.2 fold ± 1.4) and hippocampal (5.9 fold ± 1.5) tissue homogenates obtained from the aged rats (Fig. 1A, 1B, upper panel). However, the dimerization of STEP in striatal homogenates that expresses both $STEP_{61}$ and $STEP_{46}$ did not change significantly with age (Fig. 1C, upper panel). Immunoblot analysis of the same samples under reducing conditions (in the presence of β-mercaptoethanol), where disulfide bond formation cannot occur, showed only the monomeric form of STEP (Fig. 1A–C, middle panel). These findings imply that age-associated increase in oxidative stress may play a role in the dimerization of $STEP_{61}$.

3.2. Aging is associated with depletion of glutathione level and loss of activity of $STEP_{61}$

Depletion of the endogenous antioxidant, GSH has been associated with moderate to severe oxidative stress (Calabrese et al., 2000; Drake et al., 2003) and several studies have shown that both the reduced and total GSH levels decrease in many aged tissues due to increased GSH consumption and/or decreased GSH production (Maher, 2005; Ballatori et al., 2009; Emir et al., 2011; Currais and Maher, 2013). Therefore, we evaluated both the reduced and total GSH levels in cortical, hippocampal and striatal tissues obtained from young, adult and aged rats. As shown in Figure 2 (A–C) reduced GSH levels in the adult rat brains remained unaltered when compared with the younger rats. However, in the aged rats reduced GSH levels decreased considerably in both the cortex (11.6 ± 0.3 in the aged rats vs 17 ± 0.8 in

the young) and the hippocampus (13.2 ± 0.3 in the aged rats vs 16.7 ± 0.7 in the young rats). GSH level also decreased in the striatum of the aged rats but to a lesser extent (13.5 ± 0.3 in aged rats vs 14.9 ± 0.6 in the young rats) than observed in the cortex and the hippocampus. The data presented in Figure 2 (D–F) further show a substantial decrease in total GSH levels in both the cortex (13.5 ± 0.4 in aged rats vs 18.8 ± 0.9 in the young rats) and the hippocampus (13.8 ± 0.5 in aged rats vs 17.5 ± 0.8 in the young rats) of the aged rats, while in the striatum the decrease is less pronounced (13.7 ± 0.2 in aged rats vs 15.2 ± 0.5 in the young rats). These findings suggest that the depletion of both the reduced and total GSH levels vary in different brain regions and the consequences of GSH depletion on STEP dimerization depends on the GSH level.

To determine whether the increased dimerization of $STEP_{61}$ in aged rats has any effect on its phosphatase activity, STEP was immunoprecipitated from the cortex, hippocampus and striatum of young and aged rats. Tyrosine phosphatase activity of $STEP_{61}$ was measured using pNPP as a substrate and the values were normalized for the amount of $STEP_{61}$ immunoprecipitated. As shown in Figure 3 (A–C) a dramatic decrease in STEP activity was observed in the cortex (47.5 ± 3.8%) and hippocampus (40.7 ± 12.2%) of aged rats as compared with the younger controls, while in the striatum no significant change was observed.

3.3. Subcellular localization of dimerized $STEP_{61}$

To examine the sub-cellular localization of dimerized $STEP_{61}$ cortical lysates from 18-month old aged rats were subjected to biochemical fractionation (Fig. 4A). Initial studies examined the relative purity of each fraction using immunoblot analysis of marker proteins for each sub-cellular compartment (Fig. 4B). Calnexin, a calcium-binding phosphoprotein and an integral membrane protein found in endoplasmic reticulum (David et al., 1993) was highly enriched in the light membrane fraction (Fig. 4B, P3, lane 5) but not detected in the synaptosomal membrane (LP1) or synaptic vesicle-enriched (LP2) fractions. The synaptosomal membrane protein postsynaptic density-95 (PSD-95) was enriched in the crude synaptosomal membrane (P2) and synaptosomal membrane (LP1) fractions (Fig. 4B, lanes 3 and 7). The synaptic vesicle membrane protein, synaptophysin (Devoto and Barnstable, 1987), was highly concentrated in the synaptic vesicle enriched fraction (Fig. 4B, LP2, lane 9). It was also present at lower levels in the light membrane (Fig. 4B, P3, lane 5) and synaptosomal membrane (Fig. 4B, LP1, lane 7) fractions. Analysis of each fraction with anti-STEP antibody showed that $STEP_{61}$ is present in the light membrane-enriched fraction (P3), synaptosomal membrane fraction (LP1) as well as the synaptic vesicle enriched fraction (LP2). The sub-cellular fractions where $STEP_{61}$ was detected were then subjected to immunoblot analysis under non-reducing conditions. As shown in Figure 4C (lanes 4 and 7) dimerized $STEP_{61}$ was present in both the light membrane (P3) and the synaptic vesicle (LP2) enriched fractions.

3.4. Diethylmaleate induced glutathione depletion leads to dimerization of $STEP_{61}$

To evaluate more directly the effect of depleting intracellular GSH level on the dimerization of $STEP_{61}$, HEK293 cells expressing V5-tagged $STEP_{61}$ were treated with varying concentrations of diethyl maleate (DEM, 6 hr), a GSH depleting agent (Plummer et al.,

1981). Enzymatic evaluation of cellular GSH levels showed a significant dose-dependent decrease in both reduced and total GSH levels (Fig. 5A, B). Immunoblot analysis of DEM treated cell lysates, under non-reducing condition showed a concentration-dependent migration of $STEP_{61}$ to positions that correspond to double (between 100–150 kDa) and even higher molecular weights (above 150 kDa) compared with $STEP_{61}$ monomer, suggesting the formation of dimers and higher order association (oligomers). However, a significant increase in the formation of dimers and higher order oligomers of $STEP_{61}$ was observed only with the highest dose of DEM (Fig. 5C and corresponding bar diagram). To determine whether $STEP_{61}$ oligomerization following depletion of intracellular GSH levels involves intermolecular interaction, HEK293 cells expressing both V5- and myc-tagged $STEP_{61}$ were treated with varying concentrations of DEM. $STEP_{61}$-V5 was immunoprecipitated using anti-V5 antibody and co-immunoprecipitation of $STEP_{61}$-myc was determined by immunoblotting with anti-myc antibody. As shown in Figure 5D, (upper panel and corresponding bar diagram) a significant increase in co-immunoprecipitation of myc-tagged $STEP_{61}$ was observed only with the highest concentration of DEM. Re-probing the blot with anti-V5 antibody (Fig. 5D, middle panel) and immunoblot analysis of the input lysates with anti-myc antibody (Fig. 5D, lower panel) showed equal expression of both $STEP_{61}$-V5 and $STEP_{61}$-myc. To evaluate the effect of $STEP_{61}$ dimerization on its phosphatase activity, HEK293 cells expressing V5-tagged $STEP_{61}$ were treated with DEM (50 μM, 6 hr) followed by pNPP assay on immunoprecipitated $STEP_{61}$. As shown in Figure 5E a dramatic decrease in $STEP_{61}$ activity was observed in the presence of DEM (48.1 ± 1.1%) as compared with the untreated control (100 ± 1.3%). These findings provide further support for our hypothesis that decrease of cellular GSH level below a certain threshold could lead to significant increase in dimerization and subsequent loss of activity of $STEP_{61}$.

3.5. Oxidative stress induced depletion of glutathione levels and dimerization of $STEP_{61}$

Numerous studies involving both animal models of aging and elderly human subjects have suggested that increased reactive oxygen species (ROS) generation with aging is a primary contributing factor for age-associated decrease in total GSH levels (Palomero et al., 2001; Rebrin et al., 2003; Maher, 2005; Emir et al., 2011; Giustarini et al., 2011; Currais and Maher, 2013). To evaluate whether exposure to H_2O_2, the most abundant form of ROS (Poon et al., 2004; Adam-Vizi, 2005) could lead to alteration in intracellular GSH level, HEK293 cells treated with H_2O_2 (10 mM, 5 min) were processed for GSH assay. As shown in Figure 6 (A, B) H_2O_2 treatment led to a significant decrease in both reduced and total GSH levels. To examine the effect of ROS on $STEP_{61}$ dimerization HEK293 cells expressing V5-tagged $STEP_{61}$ were treated with H_2O_2 and processed for immunoblotting analysis under non-reducing conditions. As shown in Figure 6C a significant increase in $STEP_{61}$ dimerization was observed in the presence of H_2O_2. To confirm that ROS-induced $STEP_{61}$ oligomerization involves intermolecular interaction, HEK293 cells co-expressing V5- and myc-tagged $STEP_{61}$ were treated with H_2O_2 and then processed for immunoprecipitation of $STEP_{61}$-V5. As shown in Figure 6D co-immunoprecipitation of myc-tagged $STEP_{61}$ increased significantly in the presence of H_2O_2 as compared with untreated control. Taken together with the findings in Figure 5, it appears that intracellular GSH depletion either

chemically induced by DEM or resulting from oxidative stress caused by H_2O_2 could lead to dimerization of $STEP_{61}$.

3.6. Dimerization of $STEP_{61}$ involves multiple cysteine residues

In an earlier study we demonstrated that Cys 65 and Cys 76 present in the unique N-terminal domain of $STEP_{61}$ plays a role in the low level of basal dimerization of $STEP_{61}$ (Deb et al., 2010). To determine the involvement of these two cysteine residues as well as the redox-sensitive catalytic cysteine residue (Cys 472) in DEM and H_2O_2 induced dimerization of $STEP_{61}$, we generated three mutants of $STEP_{61}$. In the first mutant Cys 65 and Cys 76 were converted into serine residue (V5- and myc- tagged $STEP_{61}$ C65S/C76S), in the second mutant the catalytic cysteine residue was converted to serine (V5- and myc- tagged $STEP_{61}$ C472S) and in the third mutant all the three cysteine residues were converted to serine (V5- and myc- tagged $STEP_{61}$ C65S/C76S/C472S). HEK293 cells co-expressing the V5- and myc-tagged $STEP_{61}$ mutants were treated with DEM or H_2O_2. Co-immunoprecipitation experiments showed a significant increase in pull down of myc-tagged $STEP_{61}$ C65S/C76S with V5-tagged $STEP_{61}$ C65S/C76S following treatment with either DEM (Fig. 7A) or H_2O_2 (Fig. 7D). A similar increase in interaction was also observed between V5- and myc-tagged $STEP_{61}$ C472S (Fig. 7B and E). In contrast, mutation of all three cysteine residues (C65, C76, C472) completely abolished the increase in interaction between V5- and myc-tagged $STEP_{61}$ C65S/C76S/C472S in the presence of DEM (Fig. 7C) or H_2O_2 (Fig. 7E). This lack of intermolecular interaction between V5- and myc-tagged $STEP_{61}$ C65S/C76S/C472S suggests a role of Cys 65, Cys 76 as well as Cys 472 in the oligomerization of $STEP_{61}$.

3.7. Effect of N-acetyl cysteine on glutathione level and dimerization of $STEP_{61}$

N-acetyl cysteine (NAC), the acetylated variant of the amino acid L-cysteine and a precursor of reduced GSH has been show to enhance the intracellular biosynthesis of GSH in both *in vitro* and *in vivo* studies (Kelly, 1998; Kanwar and Nehru, 2007; Harvey et al., 2008; Prakash and Kumar, 2009). To determine whether NAC can modulate GSH levels in cortex and hippocampus, the two regions that are most affected by age, 18–20 month old aged rats were treated with NAC (50 μM) or vehicle for two weeks. This was followed by enzymatic evaluation of both reduced and total GSH levels in the cortex and hippocampus. As shown in Figure 8 (A, C) a significant increase in reduced GSH level was observed in both the cortex (13.8 ± 0.1 in the NAC treated vs 11.1 ± 0.2 in the untreated rats) and the hippocampus (14.9 ± 0.2 in the NAC treated vs 12.7 ± 0.3 in the untreated rats) following NAC treatment. Total GSH level also increased significantly in both cortex (14.3 ± 0.2 in the NAC treated vs 13.2 ± 0.2 in the untreated rats) and the hippocampus (17.1 ± 0.1 in the NAC treated vs 13.9 ± 0.3 in the untreated rats) but to a lesser extent in the cortex (Fig. 8B, D). In a parallel series of experiment NAC treated rats were processed for immunoblot analysis of cortical and hippocampal lysates under non-reducing conditions to determine the extent of $STEP_{61}$ dimerization. As shown in Figure 8 (E, F) NAC treatment resulted in a significant decrease in $STEP_{61}$ dimerization in both the cortex (59.4% ± 3.4 of control) and the hippocampus (58.9% ± 6.7 of control). Taken together the findings suggest that modulation of endogenous GSH levels can regulate $STEP_{61}$ dimerization.

4. DISCUSSION

A key finding of the current study is that depletion of endogenous GSH level with aging is associated with significant increase in dimerization of $STEP_{61}$ resulting in substantial loss of phosphatase activity. Increased dimerization of $STEP_{61}$ is particularly evident in the cortex and hippocampus of aged animals. Consistent with these findings *ex vivo* studies in HEK293 cells show that depletion of intracellular GSH level either with DEM or H_2O_2 also increase the formation of dimers and higher order oligomers of $STEP_{61}$ that involve intermolecular disulfide bond formation between multiple cysteine residues. Complementary studies in aged animals further show that increase in endogenous GSH levels by NAC supplementation reduces $STEP_{61}$ dimerization. These findings demonstrate an important mechanism of regulation of $STEP_{61}$ function *in vivo.*

Alteration in redox homeostasis is thought to be the largest risk factor for age-associated decline in cognitive and motor functions and development of both acute and chronic neurological disorders (Yankner et al., 2008; Hekimi et al., 2011). A large number of studies in both rodents and humans have shown age-associated decline in total GSH and/or reduced GSH level in the brain (Ballatori et al., 2009; Emir et al., 2011; Currais and Maher, 2013). However reduction in GSH level with aging does not necessarily involve a total loss of homeostasis but result in a shift towards more oxidative conditions. Such a pro-oxidative shift may not be always associated with a pathological condition but may disrupt redox-associated pro-survival signaling pathways, increasing the susceptibility of the aging brain to functional and metabolic stressors (Currais and Maher, 2013). Consistent with this interpretation our *in vivo* studies show that depletion of GSH level in the aging brain is associated with increased dimerization and inactivation of the brain-specific tyrosine phosphatase STEP that is known to be involved in neuroprotection (Poddar et al., 2010; Deb et al., 2013). The ability of DEM and H_2O_2 to increase $STEP_{61}$ dimerization in the *ex vivo* studies as well as the efficacy of NAC supplementation to reduce $STEP_{61}$ dimerization *in vivo* validates the role of GSH depletion in $STEP_{61}$ dimerization.

Another important finding of the present study is that although GSH level decreases significantly in the cortex, hippocampus and striatum the dimerization of $STEP_{61}$ does not increase significantly in all the three regions. A substantial increase in the dimerization of $STEP_{61}$ is observed primarily in the cortex and hippocampus and to a much lesser extent in the striatum of the aged animals. This implies that the consequences of GSH depletion depend largely upon the cellular level of GSH. Thus, a significant but relatively small depletion of GSH as observed in the striatum fails to alter the dimerization of $STEP_{61}$, while higher levels of GSH loss in the cortex and hippocampus leads to enhanced $STEP_{61}$ dimerization. The findings from DEM dose-kinetics study in HEK293 cells, demonstrating increased dimerization of $STEP_{61}$ with only the highest dose of DEM in spite of a significant depletion of GSH with all the doses of DEM tested, further support this hypothesis. Such graded response following depletion of GSH level has also been reported in an earlier study, demonstrating exponential increase in ROS generation once GSH level falls below 20% of control values (Maher, 2005). In our studies this exponential increase in ROS generation could account for the very large increase in $STEP_{61}$ dimerization observed in the cortex and hippocampus of aged animals and in the DEM treated cells, where GSH

levels fall below 20% of control values. Consistent with this view the data obtained from NAC treated animals also indicate that a ~20% increase in reduced GSH level is sufficient to limit the exponential increase in ROS resulting in substantial decrease $STEP_{61}$ dimerization in both cortex and hippocampus. Total GSH level also increases significantly in both these regions but to a lesser extent in the cortex. This could be attributed to the different metabolic conditions of the phenotypically distinct neuronal sub-population in the two regions that may result in variable uptake of NAC and synthesis of glutathione (Braak and Braak, 1994; Conrad et al., 2004; Reznikov et al., 2008). In comparison to the cortex and hippocampus, the relatively small depletion of GSH level in the striatum suggests the presence of compensatory pathways to help maintain GSH level in the aging striatum. In this context, an earlier study investigating the global gene expression profile in the cortex, hippocampus, striatum, cerebellum and spinal cord of young and aged rats observed the fewest age related changes in gene expression in the striatum and the cerebellum (Xu et al., 2007). Their findings also showed that decrease in the expression of genes related to mitochondrial function is less pronounced in the striatum and cerebellum as compared to the other three regions. This would imply a relatively efficient mitochondrial metabolic capacity and function in these two regions, which in turn could alleviate oxidative stress and GSH depletion with aging. Taken together these findings indicate region-specific changes in oxidative stress in the brain during aging, with the cortex and hippocampus being more susceptible than the striatum. Further support for this hypothesis comes from earlier studies demonstrating Ca^{2+} dysregulation and mitochondrial dysfunction in the cerebral cortex and hippocampus of the aging brain, two phenomenon that are considered direct causes of increased oxidative stress (Hartmann et al., 1996; Brown et al., 2004; Navarro et al., 2008; Navarro et al., 2011). Additional studies have also shown that both cerebral cortex and hippocampus undergo metabolic and morphological atrophy during aging in both rats and humans, which is also suggestive of oxidative damage (De Leon et al., 1997; Fjell et al., 2009).

Previous studies have indicated that oxidative stress can lead to selective oxidation of cysteine residues to sulfenic acid in a variety of proteins that includes both kinases and phosphatases, and some cysteine residues are more susceptible to oxidation than others because of their lower pKa (Paulsen and Carroll, 2010). Oxidation of such redox sensitive cysteine residues is transient as they quickly undergo further oxidation to sulfinic acid and sulfonic acid or in some cases rapidly reacts with amino acid residues in the proximity to generate secondary products. These include the formation of sulphenylamides by reaction with a neighboring peptide backbone residue and intramolecular disulfides by interacting with a proximal cysteine residue (Lo Conte and Carroll, 2013). Several *in vitro* studies have shown that such oxidative modifications of the redox sensitive catalytic cysteine residue in certain PTPs such as PTP1B, SHP-1 and SHP-2 plays a role in the regulation of their activity (Ostman et al., 2011; Lo Conte and Carroll, 2013). However, dimerization of native PTPs involving intermolecular disulfide bond formation between cysteine residues, during oxidative stress or aging, has been difficult to observe, and has mostly been reported using chimeric proteins and chemical cross-linkers in *in vitro* studies (Desai et al., 1993; Jiang et al., 1999; Walchli et al., 2005; Lee et al., 2007). In this context dimerization of $STEP_{61}$ is unique as it is readily detectable both *in vivo* as well as in cells overexpressing $STEP_{61}$

suggesting that homodimerization is an inherent property of $STEP_{61}$. The increased dimerization of $STEP_{61}$ in the microsomal and synaptic vesicle enriched fractions further indicates a shift in intracellular redox state at specific subcellular microdomains in the aged brain. The three cysteine residues involved in this aberrant increase in dimerization of $STEP_{61}$ involves the redox sensitive catalytic cysteine residue in the highly conserved phosphatase domain as well as Cys 65 and Cys 76 located in the unique N-terminal domain of $STEP_{61}$. The involvement of Cys 65 and Cys 76 in a low level of basal dimerization of $STEP_{61}$ in the absence of any stimulation has also been reported in an earlier study (Deb et al., 2011). Together, these findings indicate that the degree of oxidative stress determines the extent of STEP dimerization as well as the differential involvement of the cysteine residues in the intermolecular disulfide bond formation. Since the monomeric form of STEP is necessary for substrate binding, enzymatic activity and neuroprotective function (Deb et al., 2013), such inactivation of STEP through dimerization in the aging brain may facilitate nerve cell damage by promoting increased tyrosine phosphorylation of its physiological substrates that includes both extracellular signal-related kinase (ERK) and p38 mitogen activated protein (MAP) kinases as well as the Src-family of non-receptor tyrosine kinases.

Several studies that sought to characterize the effect of GSH depletion on intracellular signaling have shown that disruption of de novo GSH synthesis or induction of oxidative stress could trigger the activation of p38 MAP kinase (McLaughlin et al., 2001; Filomeni et al., 2003; Zhang et al., 2004; Zhang et al., 2007; Filomeni et al., 2012). Activation of p38 MAP kinase has also been identified in neurons exposed to 6-hydroxydopamine and 1-methyl-4-phenyl-1,2,3,6-tetrahydropyridine (MPTP), neurotoxins that triggers ROS production and are implicated in the mechanism of cell death (Du et al., 2001; Choi et al., 2004). *In vivo* studies in animal models of vascular dementia also showed activation of p38 MAP kinase in the hippocampus resulting in neurological dysfunction (Yang et al., 2013). Similarly a growing number of studies have established a role of ERK MAP kinase in neuronal injury following depletion of intracellular GSH level or induction of oxidative stress by H_2O_2 (Du et al., 2002; de Bernardo et al., 2004; Luo et al., 2007; Numakawa et al., 2007; Tuerxun et al., 2010). Oxidative stress caused by prolonged exposure to glutamate (5 mM) also leads to sustained activation of ERK MAP kinase that leads to caspase dependent cell death (Stanciu et al., 2000). In several studies exogenous addition of NAC has been shown to prevent activation of MAP kinases, which is consistent with a role of GSH in regulating MAP kinase function ((Yu et al., 2000; Limon-Pacheco et al., 2007). In addition to their effects on MAPKs, GSH depleting agents as well as oxidative stress inducers have also been shown to trigger activation of Src kinase (Abe et al., 2000; Yoshizumi et al., 2000; Esposito et al., 2003; McCord and Aizenman, 2014). Thus it appears that the changes in redox state in the aging brain with lowering of GSH levels may result in the activation of several kinases that are substrates of STEP. The impairment of STEP that normally functions to limit the duration of activation of ERK MAP kinase, p38 MAP kinase and Src-mediated signaling could therefore facilitate the prolonged activation of these kinases and is likely to have many unintended sequences in the aging brain.

In conclusion, the present study provides the first evidence of age-associated increased dimerization and subsequent loss of phosphatase activity of a PTP in the brain. The findings also provide new insights into the signaling mechanisms underlying oxidative stress during

aging and suggest that loss of function of STEP with aging could play a role in accelerating the progression of age-associated neurodegenerative disorders. Based on these findings subsequent studies will assess the role of STEP in modulating adaptive responses and pro-apoptotic pathways to further our understanding of the function of STEP in age-associated neurodegenerative disorders related to oxidative stress.

Acknowledgments

This work was supported by the National Institutes of Health grant numbers NS059962 to S.P. and NS065343 to R.P. We would like to thank Dr. Andrea Allan for her helpful comments.

Abbreviations

STEP	striatal-enriched phosphatase
PTP	protein tyrosine phosphatase
p38 MAPK	p38 mitogen-activated protein kinase
ERK MAPK	extracellular-regulated kinases/mitogen-activated protein kinase
GSH	glutathione
pNPP	*para*-nitrophenylphosphate
SDS	sodium dodecyl sulfate
DEM	Diethylmaleate

References

Abe J, Okuda M, Huang Q, Yoshizumi M, Berk BC. Reactive oxygen species activate p90 ribosomal S6 kinase via Fyn and Ras. The Journal of biological chemistry. 2000; 275:1739–1748. [PubMed: 10636870]

Adam-Vizi V. Production of reactive oxygen species in brain mitochondria: contribution by electron transport chain and non-electron transport chain sources. Antioxidants & redox signaling. 2005; 7:1140–1149. [PubMed: 16115017]

Ballatori N, Krance SM, Notenboom S, Shi S, Tieu K, Hammond CL. Glutathione dysregulation and the etiology and progression of human diseases. Biological chemistry. 2009; 390:191–214. [PubMed: 19166318]

Boulanger LM, Lombroso PJ, Raghunathan A, During MJ, Wahle P, Naegele JR. Cellular and molecular characterization of a brain-enriched protein tyrosine phosphatase. J Neurosci. 1995; 15:1532–1544. [PubMed: 7869116]

Braak H, Braak E. Morphological criteria for the recognition of Alzheimer's disease and the distribution pattern of cortical changes related to this disorder. Neurobiology of aging. 1994; 15:355–356. discussion 379–380. [PubMed: 7936061]

Brown MR, Geddes JW, Sullivan PG. Brain region-specific, age-related, alterations in mitochondrial responses to elevated calcium. Journal of bioenergetics and biomembranes. 2004; 36:401–406. [PubMed: 15377879]

Bult A, Zhao F, Dirkx R Jr, Raghunathan A, Solimena M, Lombroso PJ. STEP: a family of brain-enriched PTPs. Alternative splicing produces transmembrane, cytosolic and truncated isoforms. European journal of cell biology. 1997; 72:337–344. [PubMed: 9127733]

Bult A, Zhao F, Dirkx R Jr, Sharma E, Lukacsi E, Solimena M, Naegele JR, Lombroso PJ. STEP61: a member of a family of brain-enriched PTPs is localized to the endoplasmic reticulum. J Neurosci. 1996; 16:7821–7831. [PubMed: 8987810]

Calabrese V, Testa G, Ravagna A, Bates TE, Stella AM. HSP70 induction in the brain following ethanol administration in the rat: regulation by glutathione redox state. Biochemical and biophysical research communications. 2000; 269:397–400. [PubMed: 10708564]

Candelario-Jalil E, Taheri S, Yang Y, Sood R, Grossetete M, Estrada EY, Fiebich BL, Rosenberg GA. Cyclooxygenase inhibition limits blood-brain barrier disruption following intracerebral injection of tumor necrosis factor-alpha in the rat. The Journal of pharmacology and experimental therapeutics. 2007; 323:488–498. [PubMed: 17704356]

Choi WS, Eom DS, Han BS, Kim WK, Han BH, Choi EJ, Oh TH, Markelonis GJ, Cho JW, Oh YJ. Phosphorylation of p38 MAPK induced by oxidative stress is linked to activation of both caspase-8- and -9-mediated apoptotic pathways in dopaminergic neurons. The Journal of biological chemistry. 2004; 279:20451–20460. [PubMed: 14993216]

Conrad CD, Jackson JL, Wise LS. Chronic stress enhances ibotenic acid-induced damage selectively within the hippocampal CA3 region of male, but not female rats. Neuroscience. 2004; 125:759–767. [PubMed: 15099689]

Currais A, Maher P. Functional Consequences of Age-Dependent Changes in Glutathione Status in the Brain. Antioxidants & redox signaling. 2013

Dasgupta A, Das S, Sarkar PK. Thyroid hormone stimulates gamma-glutamyl transpeptidase in the developing rat cerebra and in astroglial cultures. Journal of neuroscience research. 2005; 82:851–857. [PubMed: 16302185]

David V, Hochstenbach F, Rajagopalan S, Brenner MB. Interaction with newly synthesized and retained proteins in the endoplasmic reticulum suggests a chaperone function for human integral membrane protein IP90 (calnexin). The Journal of biological chemistry. 1993; 268:9585–9592. [PubMed: 8486646]

de Bernardo S, Canals S, Casarejos MJ, Solano RM, Menendez J, Mena MA. Role of extracellular signal-regulated protein kinase in neuronal cell death induced by glutathione depletion in neuron/glia mesencephalic cultures. Journal of neurochemistry. 2004; 91:667–682. [PubMed: 15485497]

De Leon MJ, George AE, Golomb J, Tarshish C, Convit A, Kluger A, De Santi S, McRae T, Ferris SH, Reisberg B, Ince C, Rusinek H, Bobinski M, Quinn B, Miller DC, Wisniewski HM. Frequency of hippocampal formation atrophy in normal aging and Alzheimer's disease. Neurobiology of aging. 1997; 18:1–11. [PubMed: 8983027]

Deb I, Poddar R, Paul S. Oxidative stress induced oligomerization inhibits the activity of the non-receptor tyrosine phosphatase STEP(61). Journal of neurochemistry. 2010

Deb I, Poddar R, Paul S. Oxidative stress-induced oligomerization inhibits the activity of the non-receptor tyrosine phosphatase STEP61. Journal of neurochemistry. 2011; 116:1097–1111. [PubMed: 21198639]

Deb I, Manhas N, Poddar R, Rajagopal S, Allan AM, Lombroso PJ, Rosenberg GA, Candelario-Jalil E, Paul S. Neuroprotective role of a brain-enriched tyrosine phosphatase, STEP, in focal cerebral ischemia. J Neurosci. 2013; 33:17814–17826. [PubMed: 24198371]

Desai DM, Sap J, Schlessinger J, Weiss A. Ligand-mediated negative regulation of a chimeric transmembrane receptor tyrosine phosphatase. Cell. 1993; 73:541–554. [PubMed: 8490965]

Devoto SH, Barnstable CJ. Cellular and molecular biology of hormone- and neurotransmitter-containing secretory vesicles. Annals of the New York Academy of Sciences. 1987; 493:1–590. [PubMed: 2884917]

Drake J, Sultana R, Aksenova M, Calabrese V, Butterfield DA. Elevation of mitochondrial glutathione by gamma-glutamylcysteine ethyl ester protects mitochondria against peroxynitrite-induced oxidative stress. Journal of neuroscience research. 2003; 74:917–927. [PubMed: 14648597]

Droge W, Schipper HM. Oxidative stress and aberrant signaling in aging and cognitive decline. Aging cell. 2007; 6:361–370. [PubMed: 17517043]

Du S, McLaughlin B, Pal S, Aizenman E. In vitro neurotoxicity of methylisothiazolinone, a commonly used industrial and household biocide, proceeds via a zinc and extracellular signal-regulated kinase mitogen-activated protein kinase-dependent pathway. J Neurosci. 2002; 22:7408–7416. [PubMed: 12196562]

Du Y, Ma Z, Lin S, Dodel RC, Gao F, Bales KR, Triarhou LC, Chernet E, Perry KW, Nelson DL, Luecke S, Phebus LA, Bymaster FP, Paul SM. Minocycline prevents nigrostriatal dopaminergic

neurodegeneration in the MPTP model of Parkinson's disease. Proceedings of the National Academy of Sciences of the United States of America. 2001; 98:14669–14674. [PubMed: 11724929]

Dunah AW, Standaert DG. Dopamine D1 receptor-dependent trafficking of striatal NMDA glutamate receptors to the postsynaptic membrane. J Neurosci. 2001; 21:5546–5558. [PubMed: 11466426]

Emir UE, Raatz S, McPherson S, Hodges JS, Torkelson C, Tawfik P, White T, Terpstra M. Noninvasive quantification of ascorbate and glutathione concentration in the elderly human brain. NMR in biomedicine. 2011; 24:888–894. [PubMed: 21834011]

Esposito F, Chirico G, Montesano Gesualdi N, Posadas I, Ammendola R, Russo T, Cirino G, Cimino F. Protein kinase B activation by reactive oxygen species is independent of tyrosine kinase receptor phosphorylation and requires SRC activity. The Journal of biological chemistry. 2003; 278:20828–20834. [PubMed: 12682076]

Filomeni G, Rotilio G, Ciriolo MR. Glutathione disulfide induces apoptosis in U937 cells by a redox-mediated p38 MAP kinase pathway. Faseb J. 2003; 17:64–66. [PubMed: 12424221]

Filomeni G, Piccirillo S, Rotilio G, Ciriolo MR. p38(MAPK) and ERK1/2 dictate cell death/survival response to different pro-oxidant stimuli via p53 and Nrf2 in neuroblastoma cells SH-SY5Y. Biochemical pharmacology. 2012; 83:1349–1357. [PubMed: 22342995]

Fjell AM, Westlye LT, Amlien I, Espeseth T, Reinvang I, Raz N, Agartz I, Salat DH, Greve DN, Fischl B, Dale AM, Walhovd KB. High consistency of regional cortical thinning in aging across multiple samples. Cereb Cortex. 2009; 19:2001–2012. [PubMed: 19150922]

Giustarini D, Dalle-Donne I, Milzani A, Rossi R. Low molecular mass thiols, disulfides and protein mixed disulfides in rat tissues: influence of sample manipulation, oxidative stress and ageing. Mechanisms of ageing and development. 2011; 132:141–148. [PubMed: 21335026]

Hagen TM. Oxidative stress, redox imbalance, and the aging process. Antioxidants & redox signaling. 2003; 5:503–506. [PubMed: 14580304]

Hartmann H, Velbinger K, Eckert A, Muller WE. Region-specific downregulation of free intracellular calcium in the aged rat brain. Neurobiology of aging. 1996; 17:557–563. [PubMed: 8832630]

Harvey BH, Joubert C, du Preez JL, Berk M. Effect of chronic N-acetyl cysteine administration on oxidative status in the presence and absence of induced oxidative stress in rat striatum. Neurochemical research. 2008; 33:508–517. [PubMed: 17763945]

Hekimi S, Lapointe J, Wen Y. Taking a "good" look at free radicals in the aging process. Trends in cell biology. 2011; 21:569–576. [PubMed: 21824781]

Jiang G, den Hertog J, Su J, Noel J, Sap J, Hunter T. Dimerization inhibits the activity of receptor-like protein-tyrosine phosphatase-alpha. Nature. 1999; 401:606–610. [PubMed: 10524630]

Jin LW, Saitoh T. Changes in protein kinases in brain aging and Alzheimer's disease. Implications for drug therapy. Drugs & aging. 1995; 6:136–149. [PubMed: 7711360]

Jung KJ, Lee EK, Yu BP, Chung HY. Significance of protein tyrosine kinase/protein tyrosine phosphatase balance in the regulation of NF-kappaB signaling in the inflammatory process and aging. Free radical biology & medicine. 2009; 47:983–991. [PubMed: 19596065]

Kanwar SS, Nehru B. Modulatory effects of N-acetylcysteine on cerebral cortex and cerebellum regions of ageing rat brain. Nutricion hospitalaria. 2007; 22:95–100. [PubMed: 17260537]

Kelly GS. Clinical applications of N-acetylcysteine. Alternative medicine review: a journal of clinical therapeutic. 1998; 3:114–127. [PubMed: 9577247]

Kregel KC, Zhang HJ. An integrated view of oxidative stress in aging: basic mechanisms, functional effects, and pathological considerations. American journal of physiology Regulatory, integrative and comparative physiology. 2007; 292:R18–36.

Kurup P, Xu J, Videira R, Ononenyi C, Baltazar G, Lombroso PJ, Nairn AC. STEP61 is a substrate of the E3 ligase parkin and is upregulated in Parkinson's disease. Proc Natl Acad Sci U S A. 2015; 112:1202–1207. [PubMed: 25583483]

Kurup P, Zhang Y, Xu J, Venkitaramani DV, Haroutunian V, Greengard P, Nairn AC, Lombroso PJ. Abeta-mediated NMDA receptor endocytosis in Alzheimer's disease involves ubiquitination of the tyrosine phosphatase STEP61. J Neurosci. 2010; 30:5948–5957. [PubMed: 20427654]

Lee S, Faux C, Nixon J, Alete D, Chilton J, Hawadle M, Stoker AW. Dimerization of protein tyrosine phosphatase sigma governs both ligand binding and isoform specificity. Molecular and cellular biology. 2007; 27:1795–1808. [PubMed: 17178832]

Limon-Pacheco JH, Hernandez NA, Fanjul-Moles ML, Gonsebatt ME. Glutathione depletion activates mitogen-activated protein kinase (MAPK) pathways that display organ-specific responses and brain protection in mice. Free radical biology & medicine. 2007; 43:1335–1347. [PubMed: 17893047]

Lo Conte M, Carroll KS. The redox biochemistry of protein sulfenylation and sulfinylation. The Journal of biological chemistry. 2013; 288:26480–26488. [PubMed: 23861405]

Lombroso PJ, Naegele JR, Sharma E, Lerner M. A protein tyrosine phosphatase expressed within dopaminoceptive neurons of the basal ganglia and related structures. J Neurosci. 1993; 13:3064–3074. [PubMed: 8331384]

Luo J, Kintner DB, Shull GE, Sun D. ERK1/2-p90RSK-mediated phosphorylation of Na+/H+ exchanger isoform 1. A role in ischemic neuronal death. The Journal of biological chemistry. 2007; 282:28274–28284. [PubMed: 17664275]

Maher P. The effects of stress and aging on glutathione metabolism. Ageing research reviews. 2005; 4:288–314. [PubMed: 15936251]

McCord MC, Aizenman E. The role of intracellular zinc release in aging, oxidative stress, and Alzheimer's disease. Frontiers in aging neuroscience. 2014; 6:77. [PubMed: 24860495]

McLaughlin B, Pal S, Tran MP, Parsons AA, Barone FC, Erhardt JA, Aizenman E. p38 activation is required upstream of potassium current enhancement and caspase cleavage in thiol oxidant-induced neuronal apoptosis. J Neurosci. 2001; 21:3303–3311. [PubMed: 11331359]

Minetti M, Mallozzi C, Di Stasi AM. Peroxynitrite activates kinases of the src family and upregulates tyrosine phosphorylation signaling. Free radical biology & medicine. 2002; 33:744–754. [PubMed: 12208363]

Mukherjee S, Poddar R, Deb I, Paul S. Dephosphorylation of specific sites in the kinase-specificity sequence domain leads to ubiquitin-mediated degradation of the tyrosine phosphatase STEP. The Biochemical journal. 2011; 440:115–125. [PubMed: 21777200]

Navarro A, Bandez MJ, Lopez-Cepero JM, Gomez C, Boveris A. High doses of vitamin E improve mitochondrial dysfunction in rat hippocampus and frontal cortex upon aging. American journal of physiology Regulatory, integrative and comparative physiology. 2011; 300:R827–834.

Navarro A, Lopez-Cepero JM, Bandez MJ, Sanchez-Pino MJ, Gomez C, Cadenas E, Boveris A. Hippocampal mitochondrial dysfunction in rat aging. American journal of physiology Regulatory, integrative and comparative physiology. 2008; 294:R501–509.

Numakawa Y, Matsumoto T, Yokomaku D, Taguchi T, Niki E, Hatanaka H, Kunugi H, Numakawa T. 17beta-estradiol protects cortical neurons against oxidative stress-induced cell death through reduction in the activity of mitogen-activated protein kinase and in the accumulation of intracellular calcium. Endocrinology. 2007; 148:627–637. [PubMed: 17082253]

Ostman A, Frijhoff J, Sandin A, Bohmer FD. Regulation of protein tyrosine phosphatases by reversible oxidation. Journal of biochemistry. 2011; 150:345–356. [PubMed: 21856739]

Palomero J, Galan AI, Munoz ME, Tunon MJ, Gonzalez-Gallego J, Jimenez R. Effects of aging on the susceptibility to the toxic effects of cyclosporin A in rats. Changes in liver glutathione and antioxidant enzymes. Free radical biology & medicine. 2001; 30:836–845. [PubMed: 11295526]

Paul S, Nairn AC, Wang P, Lombroso PJ. NMDA-mediated activation of the tyrosine phosphatase STEP regulates the duration of ERK signaling. Nature neuroscience. 2003; 6:34–42. [PubMed: 12483215]

Paul S, Snyder GL, Yokakura H, Picciotto MR, Nairn AC, Lombroso PJ. The Dopamine/D1 receptor mediates the phosphorylation and inactivation of the protein tyrosine phosphatase STEP via a PKA-dependent pathway. J Neurosci. 2000; 20:5630–5638. [PubMed: 10908600]

Paulsen CE, Carroll KS. Orchestrating redox signaling networks through regulatory cysteine switches. ACS chemical biology. 2010; 5:47–62. [PubMed: 19957967]

Plummer JL, Smith BR, Sies H, Bend JR. Chemical depletion of glutathione in vivo. Methods in enzymology. 1981; 77:50–59. [PubMed: 7035795]

Poddar R, Deb I, Mukherjee S, Paul S. NR2B-NMDA receptor mediated modulation of the tyrosine phosphatase STEP regulates glutamate induced neuronal cell death. Journal of neurochemistry. 2010; 115:1350–1362. [PubMed: 21029094]

Poon HF, Calabrese V, Scapagnini G, Butterfield DA. Free radicals and brain aging. Clinics in geriatric medicine. 2004; 20:329–359. [PubMed: 15182885]

Prakash A, Kumar A. Effect of N-acetyl cysteine against aluminium-induced cognitive dysfunction and oxidative damage in rats. Basic & clinical pharmacology & toxicology. 2009; 105:98–104. [PubMed: 19389043]

Rebrin I, Kamzalov S, Sohal RS. Effects of age and caloric restriction on glutathione redox state in mice. Free radical biology & medicine. 2003; 35:626–635. [PubMed: 12957655]

Reznikov LR, Reagan LP, Fadel JR. Activation of phenotypically distinct neuronal subpopulations in the anterior subdivision of the rat basolateral amygdala following acute and repeated stress. The Journal of comparative neurology. 2008; 508:458–472. [PubMed: 18335544]

Schmitt TL, Hotz-Wagenblatt A, Klein H, Droge W. Interdependent regulation of insulin receptor kinase activity by ADP and hydrogen peroxide. The Journal of biological chemistry. 2005; 280:3795–3801. [PubMed: 15563471]

Stanciu M, Wang Y, Kentor R, Burke N, Watkins S, Kress G, Reynolds I, Klann E, Angiolieri MR, Johnson JW, DeFranco DB. Persistent activation of ERK contributes to glutamate-induced oxidative toxicity in a neuronal cell line and primary cortical neuron cultures. The Journal of biological chemistry. 2000; 275:12200–12206. [PubMed: 10766856]

Toledano-Katchalski H, Tiran Z, Sines T, Shani G, Granot-Attas S, den Hertog J, Elson A. Dimerization in vivo and inhibition of the nonreceptor form of protein tyrosine phosphatase epsilon. Molecular and cellular biology. 2003; 23:5460–5471. [PubMed: 12861030]

Tuerxun T, Numakawa T, Adachi N, Kumamaru E, Kitazawa H, Kudo M, Kunugi H. SA4503, a sigma-1 receptor agonist, prevents cultured cortical neurons from oxidative stress-induced cell death via suppression of MAPK pathway activation and glutamate receptor expression. Neuroscience letters. 2010; 469:303–308. [PubMed: 20025928]

Walchli S, Espanel X, Hooft van Huijsduijnen R. Sap-1/PTPRH activity is regulated by reversible dimerization. Biochemical and biophysical research communications. 2005; 331:497–502. [PubMed: 15850787]

Wegiel J, Gong CX, Hwang YW. The role of DYRK1A in neurodegenerative diseases. The FEBS journal. 2011; 278:236–245. [PubMed: 21156028]

Xu J, et al. Inhibitor of the tyrosine phosphatase STEP reverses cognitive deficits in a mouse model of Alzheimer's disease. PLoS biology. 2014; 12:e1001923. [PubMed: 25093460]

Xu X, Zhan M, Duan W, Prabhu V, Brenneman R, Wood W, Firman J, Li H, Zhang P, Ibe C, Zonderman AB, Longo DL, Poosala S, Becker KG, Mattson MP. Gene expression atlas of the mouse central nervous system: impact and interactions of age, energy intake and gender. Genome biology. 2007; 8:R234. [PubMed: 17988385]

Yang S, Zhou G, Liu H, Zhang B, Li J, Cui R, Du Y. Protective effects of p38 MAPK inhibitor SB202190 against hippocampal apoptosis and spatial learning and memory deficits in a rat model of vascular dementia. BioMed research international. 2013; 2013:215798. [PubMed: 24455679]

Yankner BA, Lu T, Loerch P. The aging brain. Annual review of pathology. 2008; 3:41–66.

Yoshizumi M, Abe J, Haendeler J, Huang Q, Berk BC. Src and Cas mediate JNK activation but not ERK1/2 and p38 kinases by reactive oxygen species. The Journal of biological chemistry. 2000; 275:11706–11712. [PubMed: 10766791]

Yu R, Mandlekar S, Tan TH, Kong AN. Activation of p38 and c-Jun N-terminal kinase pathways and induction of apoptosis by chelerythrine do not require inhibition of protein kinase C. The Journal of biological chemistry. 2000; 275:9612–9619. [PubMed: 10734112]

Zhang Y, Aizenman E, DeFranco DB, Rosenberg PA. Intracellular zinc release, 12-lipoxygenase activation and MAPK dependent neuronal and oligodendroglial death. Mol Med. 2007; 13:350–355. [PubMed: 17622306]

Zhang Y, Wang H, Li J, Jimenez DA, Levitan ES, Aizenman E, Rosenberg PA. Peroxynitrite-induced neuronal apoptosis is mediated by intracellular zinc release and 12-lipoxygenase activation. J Neurosci. 2004; 24:10616–10627. [PubMed: 15564577]

Highlights

The most important findings of the current manuscript are:

- Aging is associated with increased dimerization and loss of intrinsic phosphatase activity of the brain-enriched tyrosine phosphatase STEP.
- Increased dimerization and loss of phosphatase activity of STEP is primarily observed in the cortex and hippocampus, and strongly correlates with depletion of total glutathione level.
- Administration of N-acetyl cysteine reduces STEP dimerization both in cortex and hippocampus.
- The formation of dimers and higher order oligomers of STEP are also observed in cultured cells following glutathione depletion either chemically induced by diethylmaleate or H_2O_2 induced oxidative stress.
- Dimerization of STEP involves intermolecular disulfide bond formation involving two cysteine residues in the unique N-terminal domain and the catalytic cysteine residue.

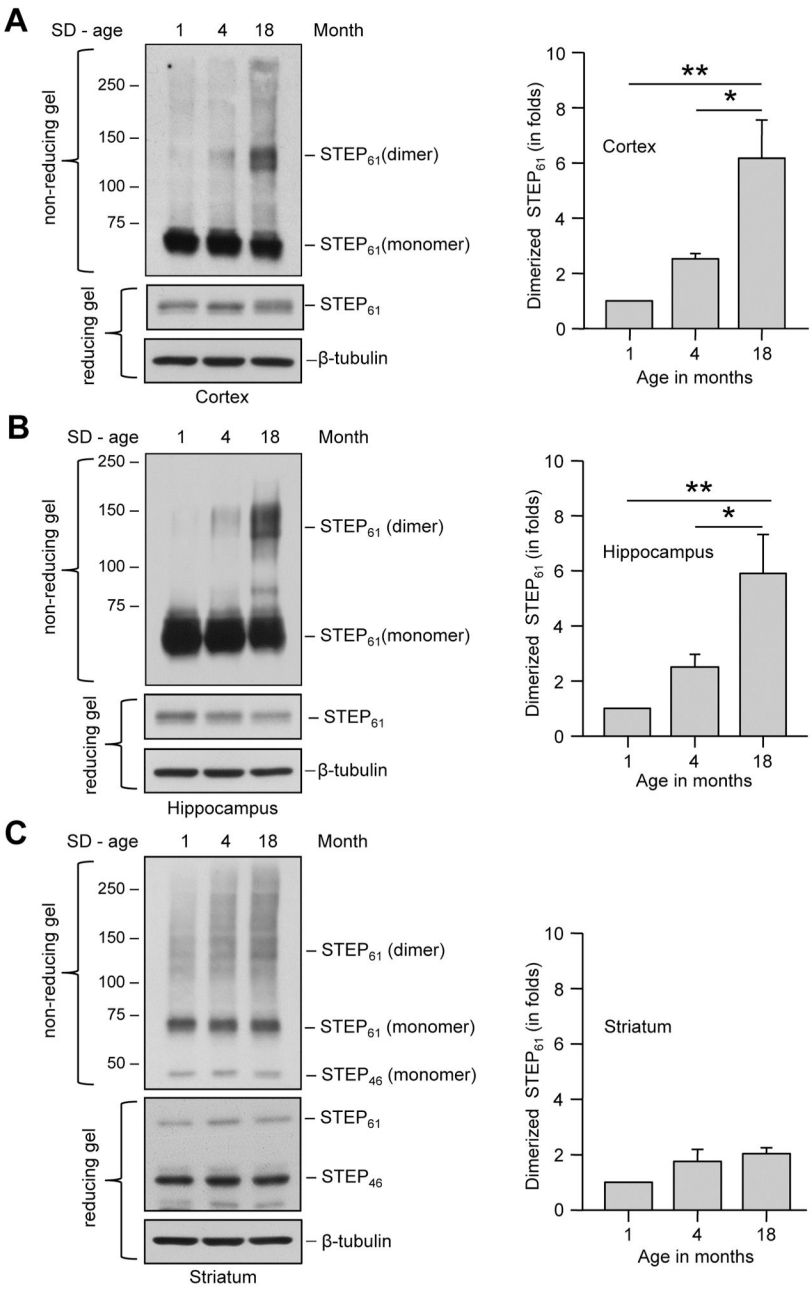

Figure 1.

Aging leads to increased dimerization of STEP in cortex and hippocampus. Equal amounts of protein from (A) cortical, (B) hippocampal and (C) striatal lysates obtained from 1, 4 and 18 month old male SD rats were processed for gel electrophoresis under non-reducing conditions (without β-mercaptoethanol) followed by immunoblotting with anti-STEP antibody to evaluate STEP dimer formation (upper panel). Equal amounts of protein from the same samples were processed under reducing conditions (with β-mercaptoethanol) to assess STEP expression level (middle panel) and the blots were re-probed with anti-tubulin antibody to indicate equal protein loading (lower panel). (A–C) Quantification of dimeric

$STEP_{61}$ in non-reducing gels (band at 100–150 kDa) was performed by computer-assisted densitometry and image J analysis (right column). Values are mean ± SEM (n = 5). *p < 0.05, **p < 0.01.

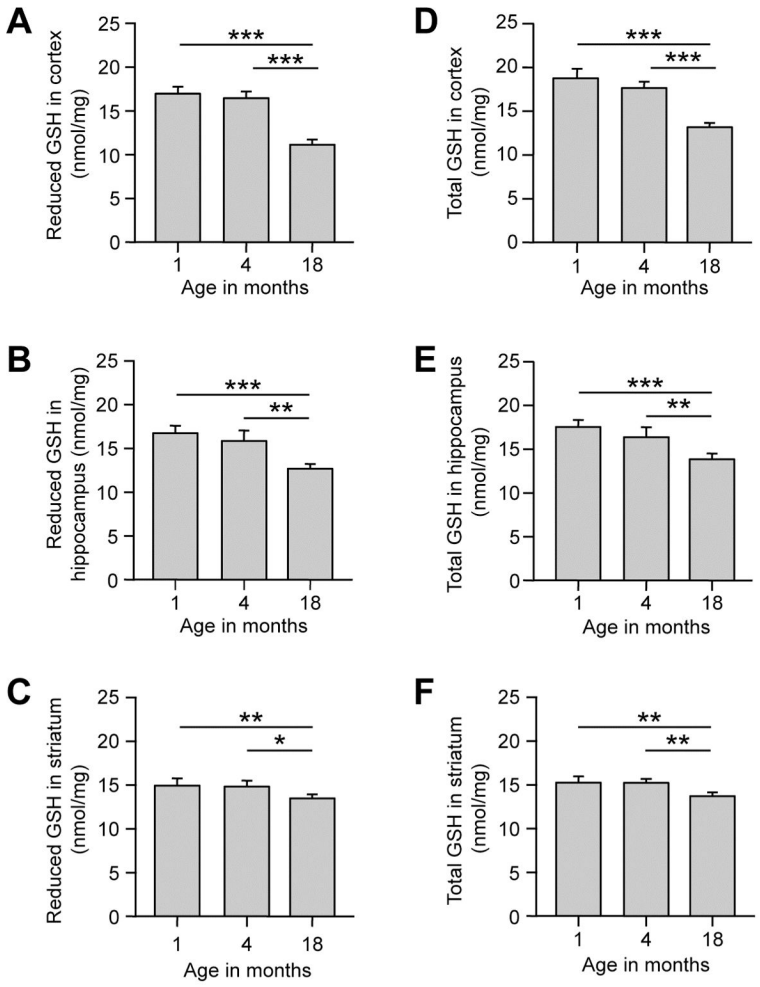

Figure 2.

Aging is associated with depletion of both reduced and total GSH levels. (A, D) Cortical, (B, E) hippocampal and (C, F) striatal lysates obtained from 1, 4 and 18 month old SD rats were processed for quantification of both reduced (A–C) and total (D–F) GSH levels. The fluorescent signal generated from the Thiostar-GSH adduct was measured fluorometrically (Ex/Em=390/510 nm). Bar diagrams represent mean ± SEM of reduced and total GSH levels (n = 5). *$p < 0.05$; **$p < 0.005$; ***$p < 0.0001$.

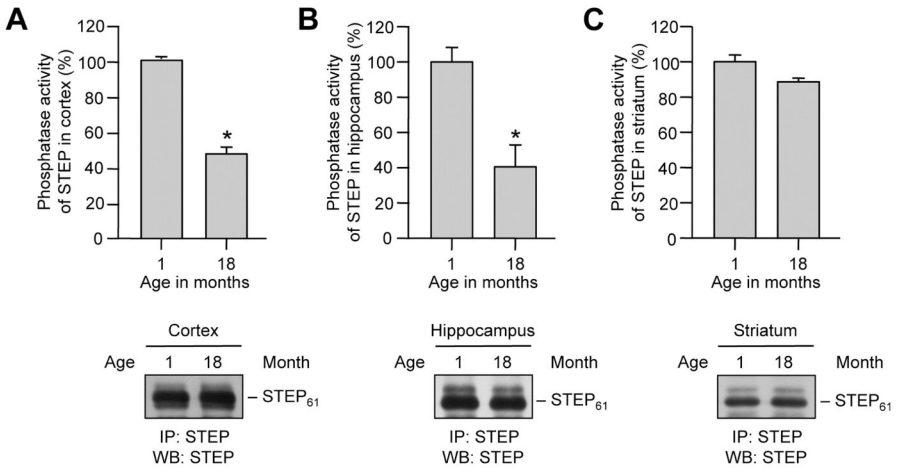

Figure 3.

Aging is associated with decrease in STEP phosphatase activity. (A) Cortical, (B) hippocampal and (C) striatal lysates obtained from 1 and 18 month old SD rats were processed for immunoprecipitation of STEP using anti-STEP antibody. PTP activity was assayed using pNPP as a substrate. Quantitative measurement of the formation of para-nitrophenolate is represented as mean ± SEM (n = 4). *$p < 0.01$. In a parallel series of experiments, immunoprecipitated STEP was subjected to immunoblotting with anti-STEP antibody. Representative immunoblots show equal pull down of STEP.

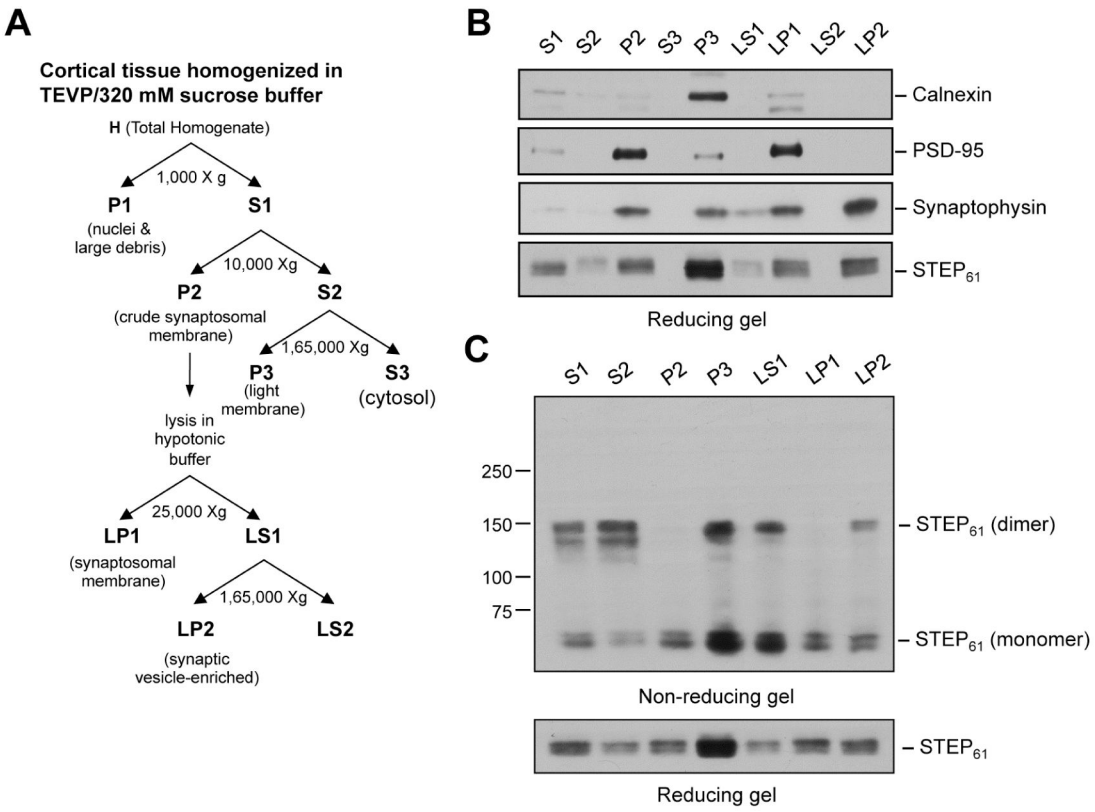

Figure 4.

Sub-cellular distribution of dimerized $STEP_{61}$ in the cortex. (A) Schematic representation of biochemical fractionation of the sub-cellular compartments in cortical homogenates. (B) Equal amounts of protein from each of the isolated biochemical fractions was processed for immunoblotting (reducing condition) with anti-calnexin (panel 1), -PSD-95 (panel 2) and -synaptophysin (panel 3) antibodies to evaluate the purity of each fraction. The sub-cellular distribution of $STEP_{61}$ in each of these fractions was evaluated using anti-STEP antibody (panel 4). (C) Protein extracts from the STEP-containing fractions were processed under non-reducing conditions to examine STEP dimer formation, using anti-STEP antibody (upper panel). The same samples were analyzed under reducing conditions to assess total STEP level (lower panel).

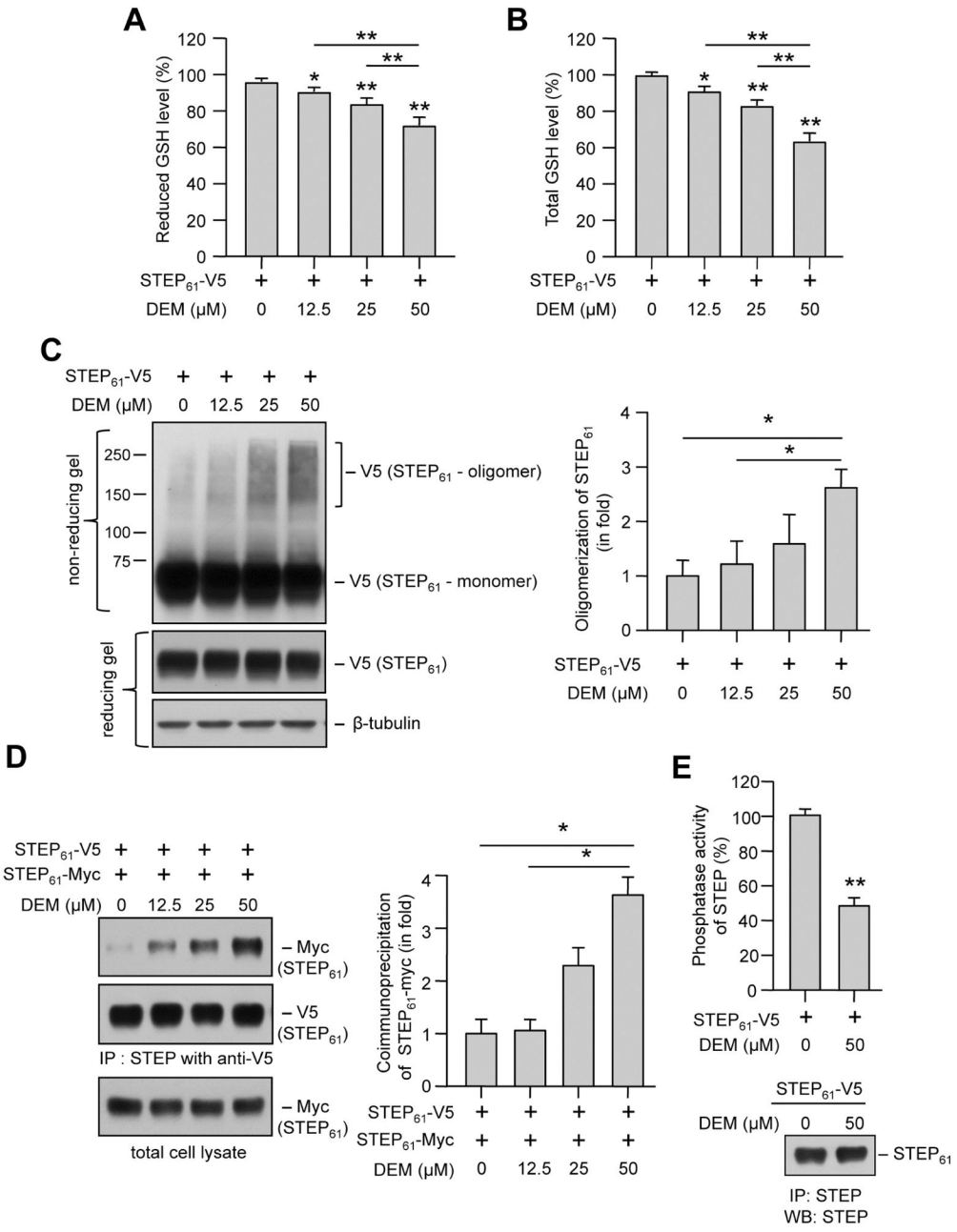

Figure 5.

DEM induced depletion of GSH levels and oligomerization of $STEP_{61}$. HEK293 cells expressing (A–C, E) V5-tagged $STEP_{61}$ or (D) V5- and myc- tagged $STEP_{61}$ were stimulated with the specified concentrations of DEM for 6 hr. (A, B) Cell lysates were processed for quantitation of reduced and total GSH levels. Bar diagram represents mean ± SEM (n = 4) of fluorescent signal in GSH assay (C) Immunoblot analysis of protein extracts from each sample under non-reducing conditions showing dose-dependent changes in STEP oligomer formation (upper panel). The same samples were analyzed under reducing conditions to assess STEP expression level (middle panel) and blots were re-probed with anti-tubulin antibody to indicate equal protein loading (lower panel). Bar diagram represent

mean ± SEM (n = 4) of oligomerized $STEP_{61}$ in non-reducing gels. (D) V5-tagged $STEP_{61}$ was immunoprecipitated with anti-V5 antibody and co-immunoprecipitation of myc-tagged $STEP_{61}$ was determined by probing with anti-myc antibody (upper panel). The blots were re-probed with anti-V5 antibody (middle panel). Expression of myc-tagged $STEP_{61}$ in total lysates was analyzed using anti-myc antibody (lower panel). Bar diagram represent mean ± SEM (n = 4) of co-immunoprecipitated myc-tagged $STEP_{61}$. (E) Phosphatase activity of $STEP_{61}$ immunoprecipitated from HEK293 cells following treatment with DEM was assessed using pNPP as a substrate. Bar diagram represents mean ± SEM (n = 5) of STEP phosphatase activity. In a parallel series of experiments immunoprecipitated $STEP_{61}$ was processed for immunoblotting with anti-STEP antibody. Representative immunoblot show equal pull down of STEP. *$p < 0.02$, **$p < 0.0001$.

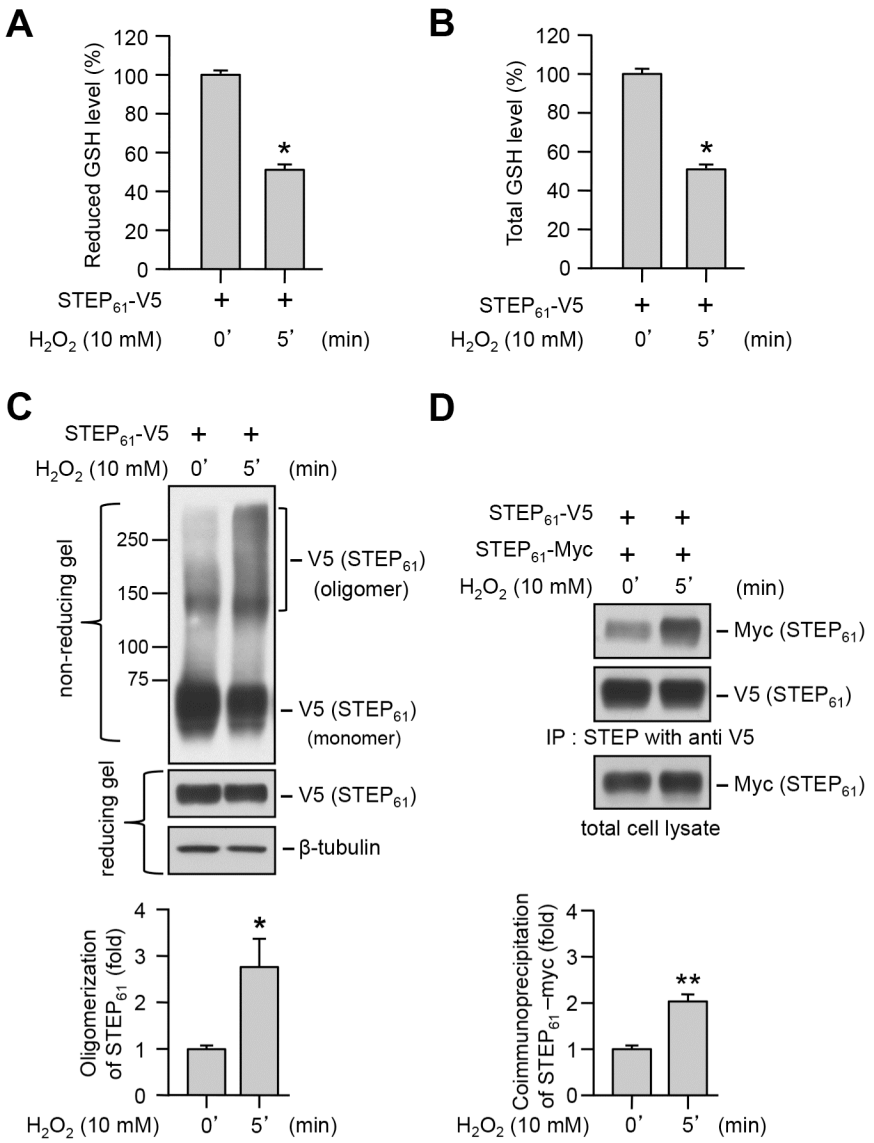

Figure 6.

Oxidative stress induced depletion of GSH levels and oligomerization of $STEP_{61}$. HEK293 cells expressing (A–C) V5-tagged $STEP_{61}$ or (D) V5- and myc- tagged $STEP_{61}$ were stimulated with H_2O_2 for 5 min. (A, B) Cell lysates were processed for quantitation of both reduced and total GSH levels. Bar diagram represents mean ± SEM (n = 4) of fluorescent signal in GSH assay. (C) Immunoblot analysis of protein extracts under non-reducing (upper panel) and reducing (middle panel) conditions to assess STEP oligomerization and expression level. Immunoblots processed under reducing conditions were re-probed with anti-tubulin antibody (lower panel). Bar diagram represent mean ± SEM (n = 4–5) of oligomerized $STEP_{61}$ in non-reducing gels. (D) V5-tagged $STEP_{61}$ was immunoprecipitated with anti-V5 antibody and co-immunoprecipitation of myc-tagged $STEP_{61}$ was determined by probing with anti-myc antibody (upper panel). The blots were re-probed with anti-V5 antibody (middle panel). Expression of myc-tagged $STEP_{61}$ in total lysates was analyzed

using anti-myc antibody (lower panel). Bar diagram represent mean ± SEM of co-immunoprecipitated myc-tagged $STEP_{61}$. *$p < 0.05$, **$p < 0.01$.

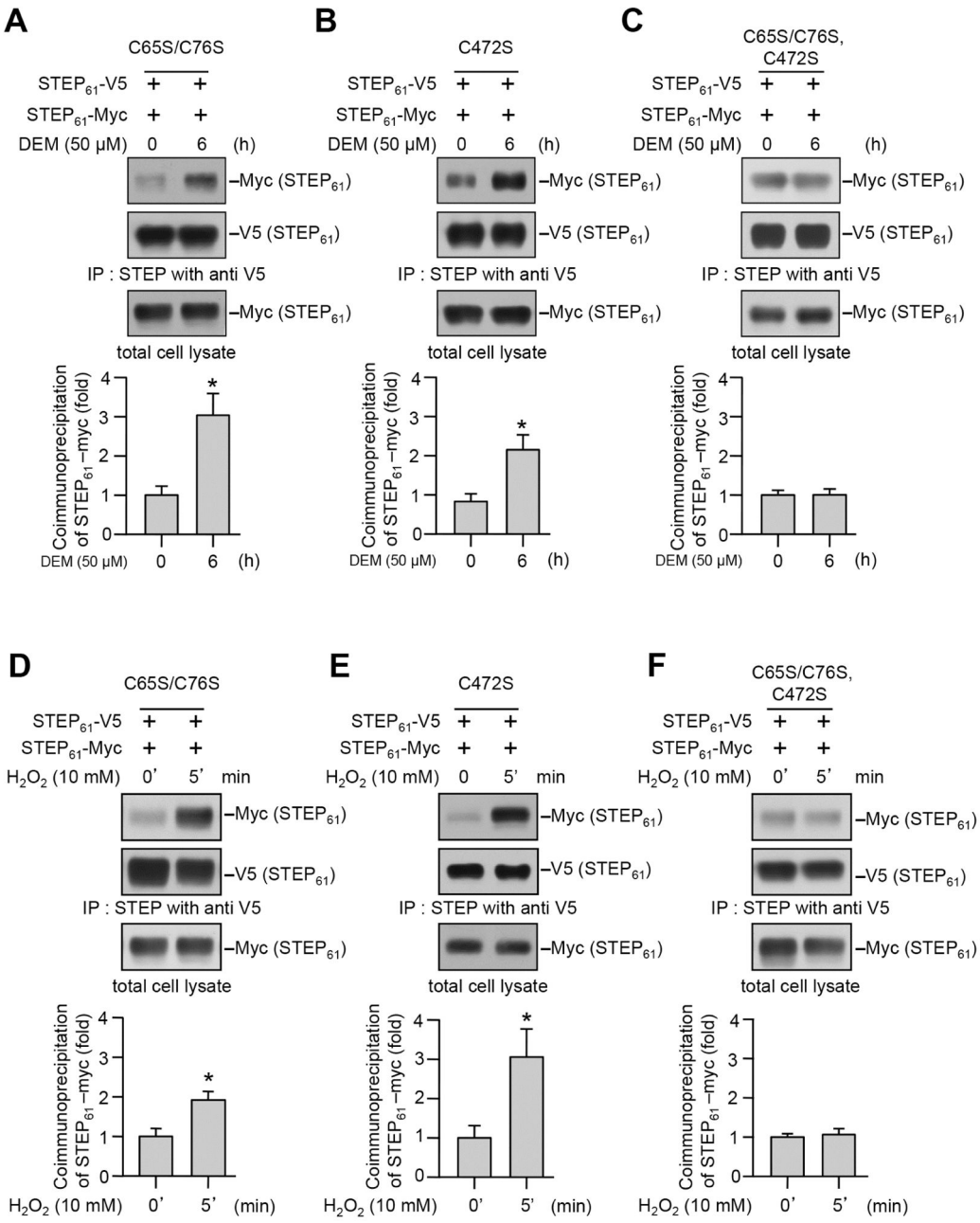

Figure 7.

Involvement of multiple cysteine residues in DEM and H_2O_2 induced dimerization of $STEP_{61}$. HEK293 cells expressing V5- and myc-tagged (A, D) $STEP_{61}$ C65S/C76S, (B, E) $STEP_{61}$ C472S or (C, F) $STEP_{61}$ C65S/C76S/C472S were treated with (A–C) DEM for 6 hr or (D–F) H_2O_2 for 5 min. V5-tagged $STEP_{61}$ was immunoprecipitated using anti-V5 antibody and co-immunoprecipitation of myc-tagged $STEP_{61}$ was determined by probing the blots with anti-myc (upper panels) antibody. The blots were re-probed with and anti-V5 antibody (middle panels). Expression of myc-tagged $STEP_{61}$ in total lysates was analyzed

using anti-myc antibody (lower panels). Bar diagram represent mean ± SEM (n = 4–5) of co-immunoprecipitated myc-tagged $STEP_{61}$. *$p < 0.05$.

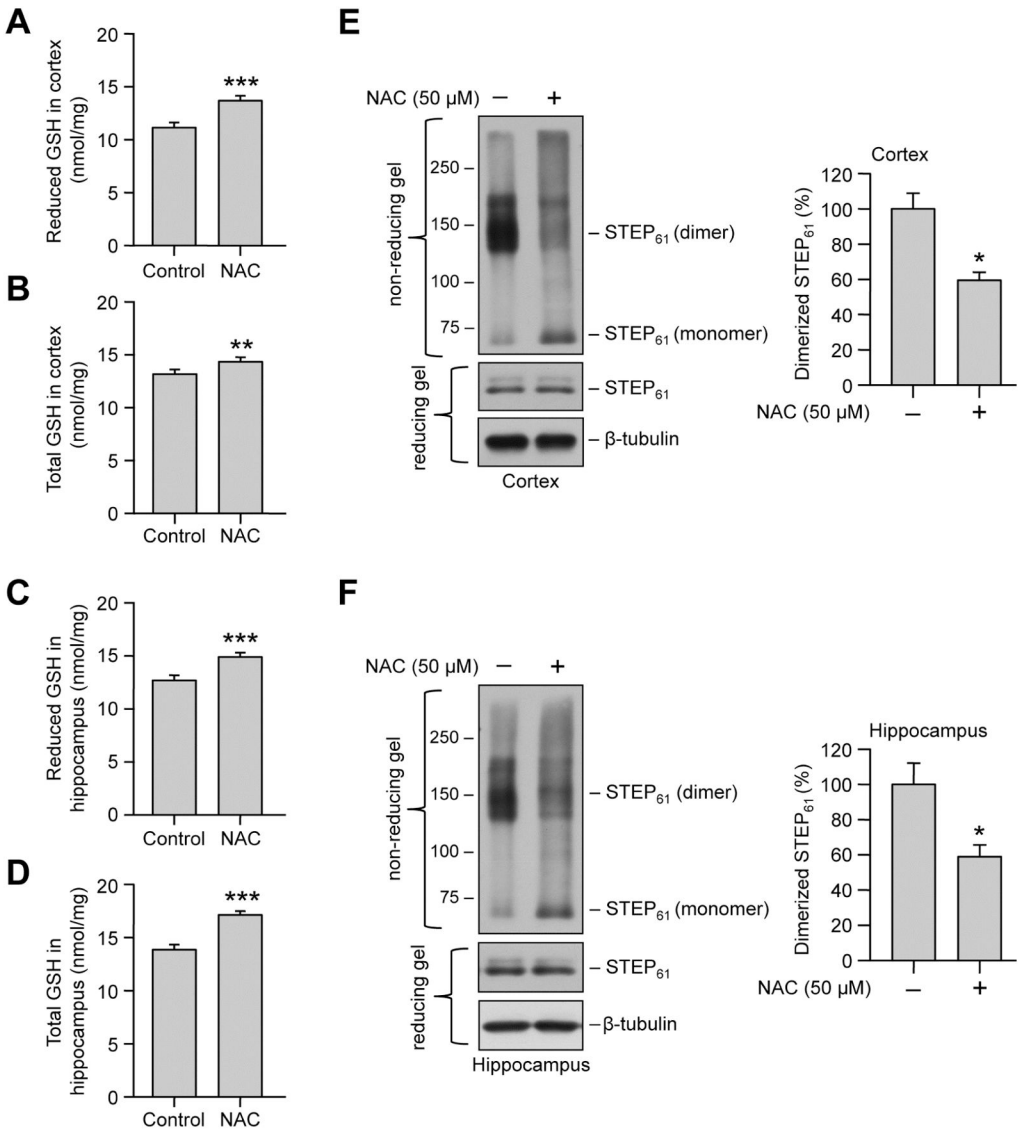

Figure 8.

Effect of N-acetyl cysteine on GSH levels and $STEP_{61}$ dimerization in cortex and hippocampus of aged rats. (A, B) Cortical and (C, D) hippocampal lysates from NAC treated rats were processed for quantification of both reduced and total GSH levels. Bar diagrams represent mean ± SEM of reduced and total GSH levels (n = 5). (E, F) In a parallel series of experiments cortical and hippocampal lysates treated with NAC were processed for immunoblot analysis under non-reducing conditions to assess STEP dimerization (upper panels). The same samples were processed under reducing conditions to assess STEP expression level (middle panels) and the blots were re-probed with anti-tubulin antibody (lower panels). Bar diagram represent mean ± SEM of dimerized $STEP_{61}$ in non-reducing gels (n = 5). *$p < 0.02$, **$p < 0.005$; ***indicates $p < 0.005$.